

Predicting plasmonic coupling with Mie–Gans theory in silver nanoparticle arrays

M. Ranjan

Received: 9 March 2013 / Accepted: 30 July 2013 / Published online: 14 August 2013
© Springer Science+Business Media Dordrecht 2013

Abstract Plasmonic coupling is observed in the self-aligned arrays of silver nanoparticles grown on ripple-patterned substrate. Large differences observed in the plasmon resonance wavelength, measured and calculated using Mie–Gans theory, predict that strong plasmonic coupling exists in the nanoparticles arrays. Even though plasmonic coupling exists both along and across the arrays, but it is found to be much stronger along the arrays due to shorter interparticle gap and particle elongation. This effect is responsible for observed optical anisotropy in such arrays. Measured red-shift even in the transverse plasmon resonance mode with the increasing nanoparticles aspect ratio in the arrays, deviate from the prediction of Mie–Gans theory. This essentially means that plasmonic coupling is dominating over the shape anisotropy. Plasmon resonance tuning is presented by varying the plasmonic coupling systematically with nanoparticles aspect ratio and ripple wavelength. Plasmon resonance red-shifts with the increasing aspect ratio along the ripple, and blue-shifts with the increasing ripple wavelength across the ripple. Therefore, reported bottom-up approach for fabricating large area-coupled nanoparticle arrays can be used for various field enhancement-based plasmonic applications.

Keywords LSPR · Plasmonic coupling · Nanoparticle arrays · Silver nanoparticles · Plasmonics · Ripple patterns

Introduction

Resonant interaction of light with coherent conduction electrons of metal nanoparticle and resulting field enhancement in the surrounding of nanoparticle have given birth to the several interesting applications, e.g. single molecule detection (Nie and Emory 1997), biological tissue detection (Qian et al. 2008) using surface-enhanced Raman scattering (SERS) phenomenon. When such resonant nanoparticles are closer enough (<50 nm), the excited plasmon modes in the individual nanoparticles interact and couple with plasmon oscillations of another adjacent nanoparticles. Such a coupled system of nanoparticles can sustain the light oscillation and allow it to travel up to several 100 nm without damping (Maier et al. 2003). Such a capability of light guiding or the so-called nanosize plasmonic waveguide has shown potential application in data transferring in a computer chip (Ozbay 2006) and in plasmonic solar cells by light trapping (Atwater and Polman 2010).

Plasmonic coupling in nanoparticles has been successfully demonstrated using various characterisation methods, e.g. Scanning Near Field Optical Microscopy (SNOM) (Maier et al. 2003; Lin et al. 2010), Electron Energy Loss Spectroscopy (EELS) (Koh

M. Ranjan (✉)
FCIPT, Institute for Plasma Research, Sector-25,
Gandhinagar, Gujarat, India
e-mail: ranjanm@ipr.res.in

et al. 2009), Dark Field illumination (DF) (Balci et al. 2011; Knight et al. 2010), Photoelectron Emission Microscopy (PEEM) (Barnes et al. 2003; Stockman et al. 2007). Also codes like FDTD (Montgomery et al. 2008; Sweatlock et al. 2005), DDA (Kooij and Poelsema 2006; Sprunken et al. 2007), and T-Matrix (Zeng and Murphy 2009) can simulate the behaviour of plasmonic coupling for the known structures and arrangements. So far there are only few experimental evidences showing plasmonic coupling in arrays of nanoparticles, most of the studies are dedicated either for two-nanoparticle system or single chain of nanoparticles (Maier et al. 2003). Usually, such arrays are produced using lithographic method and having very high interparticle gap (>70 nm) and array periodicity of several 100 nm (Jensen et al. 1999; Camelio et al. 2009; Verre et al. 2012). In the present study, existence of plasmonic coupling is shown in the case of nanoparticles dense arrays of sub 40 nm periodicity and nanoparticle gap as low as 5 nm.

Coupled-nanoparticles localised surface plasmon resonance (LSPR) occurs at a frequency that is shifted from the single nanoparticle LSPR frequency. The magnitude of frequency shift depends on the strength of the interparticle plasmonic coupling, which again depends on the proximity of the individual nanoparticles. Thus, plasmon resonance shift can be a measure of the strength of plasmonic coupling due to nanoparticles arrangement. Therefore, using this fact, coupling phenomenon is demonstrated in the case of self-aligned nanoparticles arrays grown on a ripple-patterned substrate without using conventional characterisation methods like SNOM, EELS etc. A comparison of LSPR, measured using far-field reflection measurement and analytically calculated using Mie–Gans theory (Kooij and Poelsema 2006), gives the indication that nanoparticles arrays are coupled both along and across directions. Furthermore, LSPR tuning is presented by varying nanoparticle coupling with a change in nanoparticle aspect ratio, interparticle gap and array periodicity. Demonstrating such a capability is vital to have strong field enhancement useful for SERS (Ranjan and Facsko 2012; Amendola and Meneghetti 2012; Thomas and Swathi 2012), light trapping mechanism to use such arrays as a possible bottom layer of a plasmonic solar cell (Atwater and Polman 2010), photonic waveguiding (Maier et al. 2003), and metamaterial (Oates et al. 2011).

Nanoparticles growth on ripple-patterned substrate is a rather new approach to produce nanoparticles and

nanowire arrays of desired periodicity (Ranjan et al. 2010; Oates et al. 2011; Toma et al. 2008; Babonneau et al. 2011; Verre et al. 2012). Using the above method, nanoparticle gap as low as 5 nm along the array is possible, and nanoparticle arrays can be formed over a large area. Such kinds of ordered arrays of nanoparticles are also reported using stepped surfaces, but with a much higher array periodicity of around 200 nm (Camelio et al. 2009; Verre et al. 2012). However, in all such cases, only one set of array periodicity is reported unlike in the present study, where nanoparticles of different aspect ratios with different array periodicities of much lower dimension (20, 30 and 45 nm) are reported. Since plasmonic coupling decays very fast above 20 nm, forming arrays of very narrow dimension is important for any plasmonic application (Su et al. 2003; Jain et al. 2007).

Such arrays of nanoparticles are optically anisotropic, i.e. along and across the array there exists different LSPR (Ranjan et al. 2010; Oates et al. 2011; Toma et al. 2008). Due to differences in localised dielectric coefficients along x, y and z-axis, such nanoparticle and nanowire arrays known to have biaxial optical anisotropy (Ranjan et al. 2010; Oates et al. 2011). Observed optical anisotropy or different dielectric coefficients in such self-assembled nanoparticles/nanowires arrays is either due to the shape of nanoparticles or due to the different plasmonic coupling or due to both effects. (Camelio et al. 2009) presented the effect of shape of nanoparticles using effective dielectric coefficient. As of today study about the plasmonic coupling of self-assembled nanoparticle on ripple-patterned substrate is not reported. As mentioned earlier, in the present study based on measured and calculated LSPR, it is clearly demonstrated that nanoparticles aligned on ripple-patterned substrate are coupled irrespective of the nanoparticle shape. Anisotropic coupling of particles is found to be responsible for observed optical anisotropy and much more dominating than shape anisotropy. Finally, tuning of LSPR will be shown by varying the plasmonic coupling with the help of experimental parameters.

Experimental

A bottom-up, two-step process has to be followed to produce nanoparticle and nanowire arrays using ripple-patterned substrate as shown in Fig. 1. In the

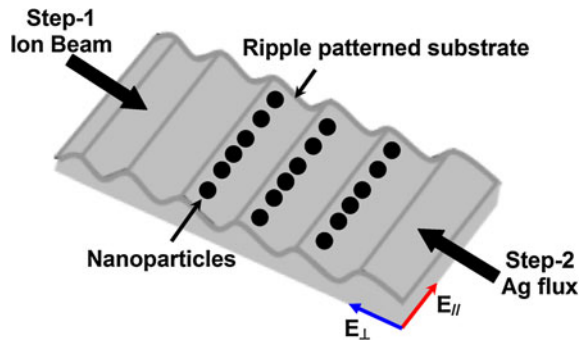


Fig. 1 Two-step process of making ripple-patterned substrate and then growing self-aligned nanoparticles. Also shown is the direction of polarised light electric field exciting plasmon; along the ripple (red), and across the ripple (blue), respectively. (Color figure online)

first step, ripple-like pattern of shallow modulation (~ 2 nm) are produced by ion irradiations, and in the second step, grazing incidence PVD growth is performed perpendicular to the ripple direction (Oates et al. 2011; Toma et al. 2008; Babonneau et al. 2011; Verre et al. 2012; Ranjan et al. 2012). At an optimised angle of incidence, energy and fluence, such ripple-like pattern evolves in a self-organised process due to simultaneous occurrence of surface diffusion and surface erosion phenomenon (Keller et al. 2008). Ion energy and fluences provide a great amount of liberty to tailor the ripple periodicity starting roughly from 20 nm to several 100 nm. As mentioned already, plasmonic coupling is very strong below 20 nm (Su et al. 2003; Jain et al. 2007), and therefore, ripple of 20, 30, 35, and 45 nm periodicities were produced on Si (100) surface to form nanoparticles dense arrays. In this case, Ar ions beam was incident at an angle of 67° , ion energy was kept at 500 eV, and fluence was varied from $5 \times 10^{16} \text{ cm}^{-2}$ to $7 \times 10^{17} \text{ cm}^{-2}$ to prepare the ripple patterns of various wavelengths on Si substrate. After the ion bombardment and exposure to atmosphere, a layer of ~ 5 -nm-thick SiO_2 forms on top of Si (Fig. 2c). This results in increasing interfacial energy between silver and substrate and promotes Volmer–Weber (V.W) growth mode (Numazawa et al. 2011).

PVD e-beam evaporation was used for deposition along the normal to the ripple direction at an angle 20° with respect to the surface (Ranjan et al. 2012). In the initial phase, several small size nanoparticles grow on the ripple surfaces following the V.W growth mode and then eventually coalescence process begin to form

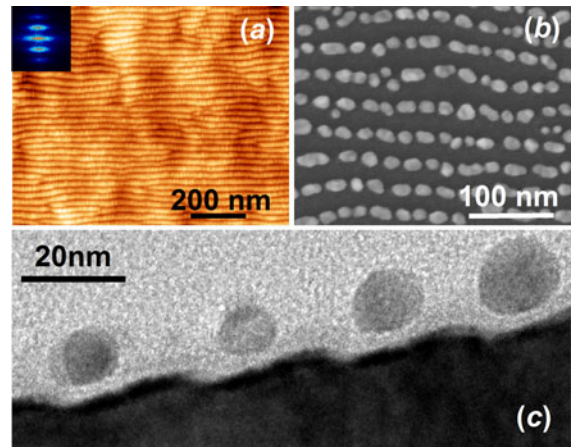


Fig. 2 **a** AFM image of the ripple-patterned substrate; *inset* shows the FFT of the surface. **b** SEM image of the ordered silver nanoparticles. **c** Cross-sectional TEM of the aligned nanoparticles on the ripple-patterned substrate

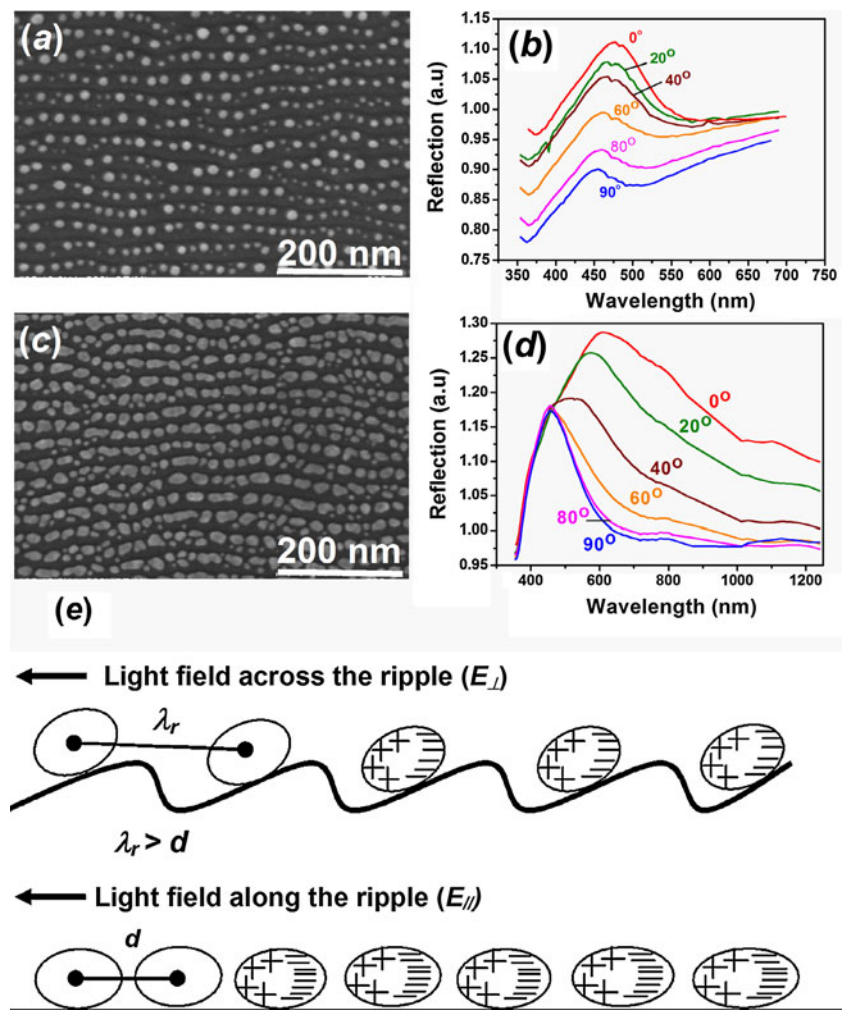
higher aspect ratio nanoparticles (Numazawa et al. 2011). Therefore, in a longer time regime, nanoparticles length mainly changes along the ripple compared with its width across the ripple. Nanoparticle arrays of aspect ratio of 2–5 were prepared mainly by varying the deposition time and annealing temperature. To obtain nearly spherical-shaped nanoparticles, samples were post annealed at 300°C so that they attain thermodynamically favourable spherical shape (Ranjan et al. 2013; Ranjan et al. 2012). Likewise, arrays of different periodicities and aspect ratios nanoparticles were produced.

Examples of tapping-mode AFM image of the studied ripple-patterned sample and SEM images of nanoparticles arrays are shown in Fig. 2a and b, respectively. Inset of Fig. 2a shows the Fast Fourier Transformation (FFT) of the surface, with two intense peaks clearly representing the long-range ordering of ripple patterns. It can be observed in the SEM and TEM images (Fig. 2c) that nanoparticles are perfectly aligned along and across the ripple template. A capping layer of Boron Nitride (BN) was used to prevent nanoparticles shape deformation for the cross-sectional TEM measurement.

LSPR measurements

LSPR was observed in a reflection measurement using an Ellipsometer. Polarised light was incident near

Fig. 3 Ordered spherical nanoparticles and corresponding reflection spectra at various azimuthal rotations (a) and (b), respectively. Ordered elongated nanoparticles and corresponding reflection spectra at various azimuthal rotations (c) and (d), respectively. e Schematic diagram of ordered nanoparticles along and across the ripple showing different interparticle gaps and light electric fields along and across the ripple



normal incidence, along and across the array. Polarised light-exciting plasmon along the ripple (E_{\parallel}) is designated as longitudinal plasmon and across the ripple (E_{\perp}) as transverse plasmon, respectively. Initially, light polarisation was aligned parallel to the ripples; later, sample was rotated azimuthally in the steps of 20° with respect to the incident polarised light from along the ripples (0°) to across the ripple (90°). Corresponding reflection spectra for spherical and elongated nanoparticles arrays are shown in Fig. 3a and b, respectively. Spherical nanoparticles generate a sharp resonance peak at plasmon frequency, and LSPR blue-shifted from 475 nm along the ripple to around 450 nm across the ripple. Along the ripple, LSPR of elongated nanoparticle is red-shifted in comparison with spherical nanoparticles (Fig. 3b), and the reflection intensity is also higher. This indicates that

elongated nanoparticles have stronger plasmonic coupling compared with spherical nanoparticles. In the case of elongated nanoparticles, LSPR is again blue-shifted from 600 nm along the ripple to 450 nm across the ripple. This shift is larger compared with spherical nanoparticles. Broadening of the LSPR spectra drastically reduces across the ripple in both the cases, indicating that nanoparticles shape distribution is more along the ripple. In both the cases presented here, LSPR across the ripple occurs at 450 nm; this means that a preferential silver growth across the ripple significantly changes the nanoparticle elongation, but not the width.

It is obvious from the reflection spectra that these samples are strongly anisotropic, i.e. LSPR is changing with direction of incident light field. In the case of nearly spherical nanoparticles (Fig. 3a), based on

nanoparticles size statistics, shape anisotropy is negligible, but still a large shift of 25 nm in plasmon resonance is observed. This indicates that, it is not the shape but different plasmonic couplings along and across the ripples which is responsible for the observed anisotropy. Along the ripple, the interparticle gap is roughly 10 nm, and across the ripple, particles are separated by ripple wavelength of 35 nm as shown in Fig. 3e. Therefore, due to different interparticle gaps along and across the ripple, plasmonic coupling is affected, which leads to the optical anisotropy. A sample of non-ordered nanoparticles was also prepared on ripple-patterned substrate by performing deposition normal to the surface (Ranjan et al. 2013; Ranjan 2012). In this case, no direction-dependent shift in LSPR was observed due to isotropic plasmonic coupling. Therefore, anisotropy is originated when nanoparticles are in an ordered form over the ripple-patterned substrate.

It has been found experimentally as well as theoretically that the plasmonic coupling vanishes exponentially with interparticle gap (Su et al. 2003; Jain et al. 2007). The light scattering theory (Chern et al. 2007) demonstrated that the plasmonic coupling also increases with the number of nanoparticles arranged in a row. The number of aligned nanoparticles is higher along the ripple compared with the perpendicular direction. More number of nanoparticles with lesser interparticle gap couple strongly and consequently make a larger red-shift. Therefore, it is also visible in Fig. 3b and d that the resonance strength perpendicular to ripple direction is weaker than that parallel to it. Interparticle gap and the number of nanoparticles along and across the ripple affect the plasmonic coupling and result in the anisotropy.

Comparison with Mie–Gans theory

Study presented for one set of nanoparticles was also extended to nanoparticle arrays of different aspect ratios. The aspect ratio was varied between 2 to 5 in our experiments. Nanoparticles become elongated in shape with the increasing aspect ratio. LSPR of all these samples are shown in Fig. 4a and b both along and across the ripple, respectively. Correspondingly, calculated LSPR values of all samples according to Mie–Gans theory are also compared in Fig. 4a and b,

respectively. Gans theory is the extended Mie theory for the elongated or rod-like structures and applicable for single-particle treatment (Kooij and Poelsema 2006; Azarian et al. 2008). It states that in elongated nanoparticles, plasmon can be excited in two directions—along the length (longitudinal plasmon) and along the width (transverse plasmon). Plasmon excited in the longitudinal direction also excites higher-order weak plasmon in the transverse direction, and as a result, two resonance peaks appear (Krenn et al. 2000). In our reflection measurement, only single LSPR peak corresponding to longitudinal plasmon was observed for any set of aspect ratios used for this study. This confirms that plasmons are independently excited along and across the ripple.

Under quasi static dipole approximation, if dielectric coefficient of surrounding and bulk metal is known, Gans theory gives the Eq. (1).

$$\epsilon_{1(\text{metal})} = -k_i \epsilon_m \tag{1}$$

$\epsilon_{1(\text{metal})}$ and ϵ_m are the real dielectric coefficients of bulk metal and surrounding media, respectively. ϵ_m is the effective dielectric coefficient of medium due to Air and SiO₂ substrate surface. Small portion of the nanoparticles (~5 %) is in contact with the SiO₂ surface, and the rest ~95 % is in Air (Fig. 2c). Therefore, as an approximation, ϵ_m is calculated considering the above percentage weight, i.e. $\epsilon_m = (95 \% \text{ of } \epsilon_{\text{air}} + 5 \% \text{ of } \epsilon_{\text{SiO}_2})$. In this way, the value of ϵ_m is calculated to be 1.12. k_i is the space-dependent screening geometrical factor given by.

$$k_i = (1 - p_i)/p_i \quad i = x, y, z \tag{2}$$

$$p_x = p_y = (1 - p_z)/2 \tag{3}$$

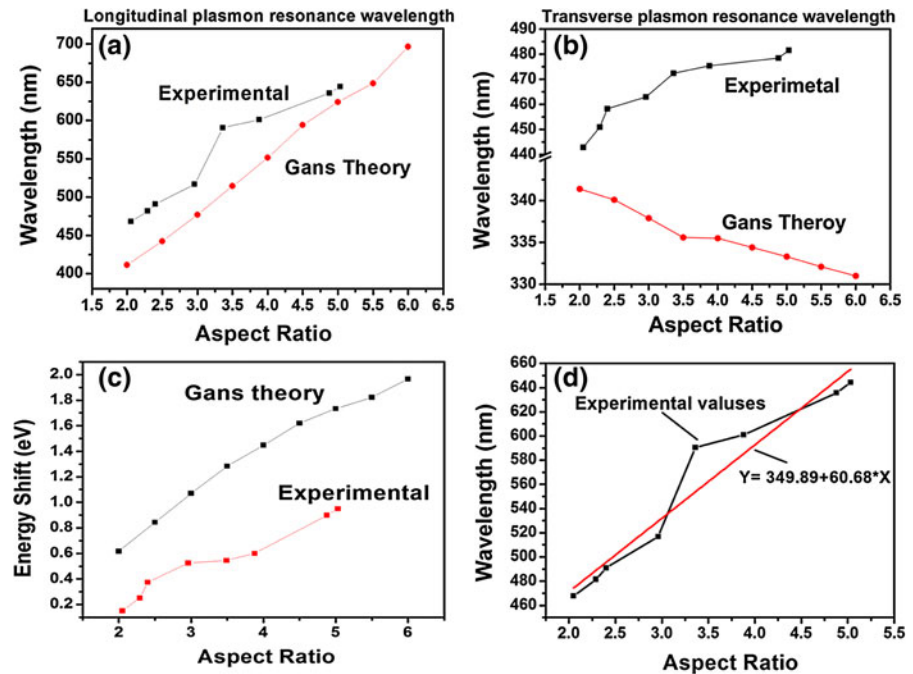
$$p_z = (1 - e^2)[\ln(((1 - e)/(1 + e)) - 2e)]/2e^3 \tag{4}$$

$$e = [(l^2 - d^2)/d^2]^{1/2} \quad l/d \text{ is aspect ratio} \tag{5}$$

The x and y axes are nearly identical and correspond to the nanoparticle diameter (d), whereas the z axis represents the elongated length (l).

Calculated dielectric functions along longitudinal and transverse plasmon resonance mode for all the samples are compared with existing silver metal data base (Kreibig and Vollmer 1993; Johnson and Christy 1972; Hsu et al. 1983). This means under resonance condition using Eq. (1) ($\epsilon_{1(\text{metal})} = -k_i \cdot \epsilon_m$), the dielectric functions depends on geometrical function (k_i) and embedding medium (ϵ_m). Since k_i depends on

Fig. 4 **a** Calculated and experimentally measured LSPR values corresponding to longitudinal plasmon. **b** Calculated and experimentally measured LSPR values corresponding to transverse plasmon. **c** Calculated and measured energy shifts. **d** Fitted straight line in the LSPR value measured at different aspect ratios. All the plots (a–c) are plotted for different aspect ratios



nanoparticles aspect ratio, dielectric functions are easy to calculate. Dielectric functions provide the corresponding wavelength at which LSPR occur and that can be easily obtain from silver metal data base. Calculated LSPR peak wavelength is then compared with the experimentally obtained values as shown in Fig. 4a and b for longitudinal and transverse plasmon excitation, respectively.

It is worth to note that the wavelength of longitudinal plasmon resonance follows the trend like Gans theory, i.e. wavelength corresponding to LSPR is red-shifted with the increasing aspect ratio. The largest difference between measured and calculated value is within 25 nm (Fig. 4a). However, in transverse plasmon mode, this difference is more than 100 nm (Fig. 4b). With the increasing nanoparticles length along the ripples, the number of nanoparticles and their interparticle gap is reduces. Therefore, with increasing aspect ratio deviation between experimentally observed longitudinal LSPR peaks and predicted by Gans theory is also reduced (Fig. 4a). Gans theory is valid for single nanoparticle treatment only and we are comparing it for nanoparticles chain. Therefore, when the number of nanoparticles is reduced deviation between theory and experimental values also reduces. With the increasing length, more nanoparticle coalescence and move towards single particle behaviour, i.e.

for single nanoparticle case theory and experiment should nearly coincide. This deviation between calculated and measured LSPR clearly indicates the nanoparticles aligned on ripple-patterned substrate are coupled. Also since this deviation observed in both the direction which again confirms that nanoparticles are coupled both along and across the array depending on the excitation.

In the case of single nanoparticle, Gans theory predicts a blue-shift in the transverse mode plasmon resonance with the increasing aspect ratio (Azarian et al. 2008; Zong et al. 2004), but in our measurements a red-shift is observed in this case (Fig. 4b). This red-shift even increases with aspect ratio like in the case of longitudinal plasmon. This trend can be explained with the following argumentation, Gans theory predicts blue-shift in the transverse direction due to different shape of nanoparticle. In our samples as well, nanoparticles shape is changing across the ripple with the increasing aspect ratio but as compared to shape effect, plasmonic coupling in between the nanoparticles is much stronger. With aspect ratio the width of particles is also increasing, which reduces the interparticle gap across the ripple even though ripple wavelength is fixed. Thus, coupling in between two adjacent nanoparticles appears to be dominating over the shape effect of individual nanoparticle and hence

results in a red-shift in LSPR even in transverse plasmon resonance.

Here it is important to note that due to ripple tilt or irregularity at some places, nanoparticles are not perfectly aligned. Therefore, when plasmons are excited in the transverse direction, there is a possibility that longitudinal plasmon may also excite and contribute to the red-shift in LSPR. Such misaligned nanoparticles may also develop quadruple excitation, but as mentioned earlier, no higher-order peaks are observed in our LSPR measurement in either direction. If LSPR is probed locally, there may be a variation at different special locations in the proximity of nanoparticles. In the present study, LSPR is observed using reflection measurement, which follows a far-field measurement technique and captures the averaged out information. Different kinds of misalignments (nanoparticles tilt on the axis of alignment, nanoparticles tilt in between two nanoparticles arrays etc.) may contribute to both red and blue shift in the LSPR. Such contributions are expected to be negligible but can not be rule out completely. Since this would require complete information (Number, angle of tilt, interparticle gap) of such nanoparticles to incorporate in the calculation, which is not possible simply using Mie–Gans theory presented in this study. However, plasmonic coupling will be stronger if all the particles are perfectly aligned.

A very important observation is that when the aspect ratio changes from 2 to 5, the red-shift in longitudinal direction is very high (~ 150 nm) while in transverse direction it is only ~ 40 nm. This also confirms the prediction of other reported study that coupling is stronger along the particle long axis and is distance dependent (Su et al. 2003; Jain et al. 2007). Due to larger shift along the ripples, a larger difference in energy shift is found compared to the calculated values by Gans theory (Fig. 4c). Due to the preferential growth along the ripple mainly the length of the particles is changed and the width is almost constant. Therefore, the resonance peak wavelength corresponding along the ripple is more strongly red-shifted compared with across the ripple. This increases the energy shift with increasing aspect ratio. However, again there is a large difference with the values predicted by Gans theory due to the plasmonic coupling of nanoparticles. So Gans theory is only in qualitative agreement with our results; however, due to plasmonic coupling as mentioned above, there are discrepancies.

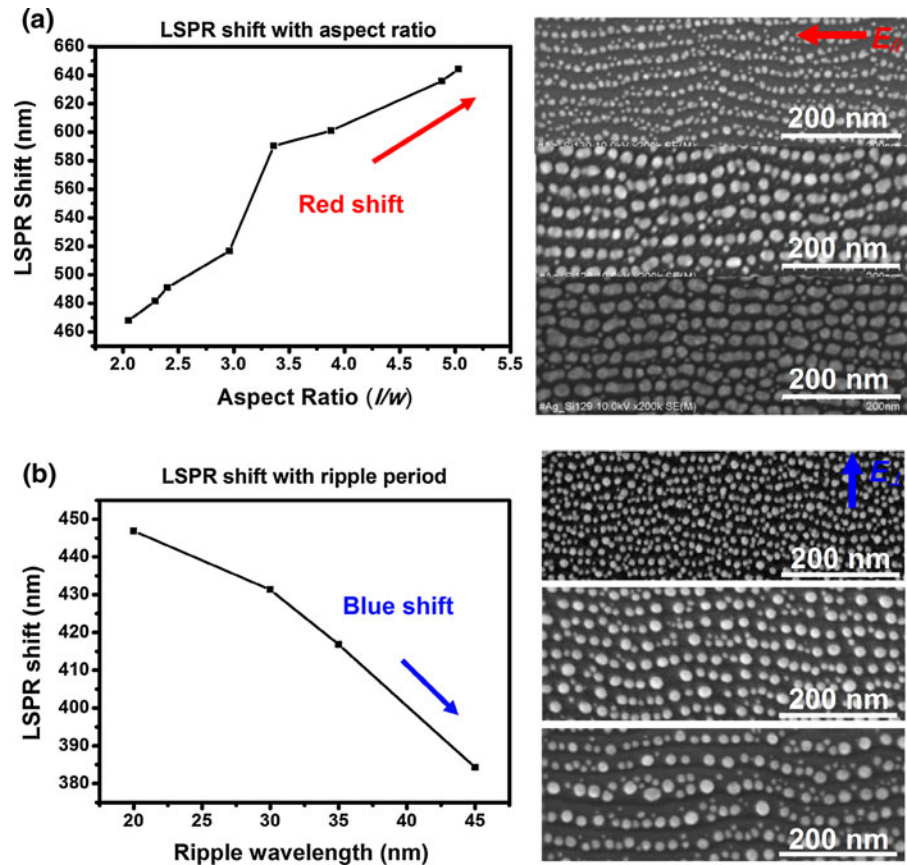
LSPR tuning

In Fig. 4d, the variation in peak longitudinal wavelength is plotted against aspect ratio and a straight line is fitted to the plot. Usually, in the literature LSPR peak wavelength is reported with a straight line fit to express the tunability of LSPR with aspects ratio (Sprunken et al. 2007; Brioude et al. 2005). So for the sake of completeness straight line fitted in our case is also shown here (Eq. 6), which is quite similar compared with other reported study of similar nature (Sprunken et al. 2007; Brioude et al. 2005). So even in nanoparticles arrays plasmon resonance tunability with aspect ratios follows straight line dependency.

$$\begin{aligned} (\text{Peak Wavelength}) \text{ nm} &= (60.68) \text{ nm} \\ &\times (\text{Aspect ratio}) + 349.89 \text{ nm} \end{aligned} \quad (6)$$

It is mentioned earlier that ripple of different periodicities can be produced using ion energy and fluence. Also by varying the growth parameters, silver nanoparticles of different aspect ratios can be produced. These two factors provide a great amount of flexibility to tune the plasmon resonance and directly affect the nanoparticles plasmonic coupling. Examples of tuning the LSPR using self-aligned nanoparticles on pre-patterned ripple surfaces are shown in Fig. 5a and b. Nanoparticles of various aspect ratios grown on a fixed array periodicity of 35 nm is shown in Fig. 5a, and for nearly the same sized spherical nanoparticle, arrays of 20, 35 and 45 nm periodicity are shown in Fig. 5b. It is already discussed that the increasing aspect ratio red-shifts the plasmon resonance along the ripples, as shown in Fig. 5a. Across the ripples, interparticle gap is mainly determined by the ripple wavelength. When the ripple periodicity increases from 20 to 45 nm, a clear blue-shift in LSPR is observed. Even though the average nanoparticle size is slightly smaller in the case of 20 nm periodic array, still they show the highest shift due to strong plasmonic coupling. This is a clear evidence showing the effect of interparticle distance on plasmonic coupling. Both the factors reported here, i.e. aspect ratio and interparticle gap, are important, which change the coupling substantially. In addition, by performing the annealing at different temperatures and times, interparticle gap along the ripple can also be adjusted. During annealing, not only the interparticle gap is changed, but also the number of nanoparticles due to Ostwald ripening. Therefore, LSPR along the

Fig. 5 **a** Red-shift in longitudinal LSPR with the increasing aspect ratios of nanoparticles is shown in the SEM images. **b** Blue-shift in LSPR with the increasing periodicity of the ripples for spherical nanoparticles of nearly the same size. (Color figure online)



ripples can also be tuned by changing the number of nanoparticles. In this way, it is demonstrated that nanoparticle arrays grown on ripple-patterned template provide a great amount of flexibility for tuning the LSPR by means of changing plasmonic coupling with different experimental parameters.

Conclusions

In conclusion, it is shown here that Mie–Gans theory can be used to see if nanoparticles are coupled or not. Coupling in closely arranged nanoparticles is a more dominating phenomenon than the shape anisotropy. Coupling is a strong function of nanoparticles aspect ratio and interparticle gap in nanoparticle arrays. Therefore, the above presented method of producing nanoparticle array using ripple-patterned template provides immense flexibility toward the tunability of the plasmonic coupling by varying the nanoparticles aspects ratio and ripple periodicity. Such a capability of large area production of metallic nanoparticle arrays can be used

in various applications such as SERS-based molecular sensing (Ranjan and Facsko 2012; Amendola and Meneghetti 2012; Thomas and Swathi 2012) and light trapping in plasmonic solar cell (Atwater and Polman 2010). Such a narrow gap array with strong plasmonic coupling can produce strong field enhancement and can also entrap the light. This can give a better sensitivity in SERS measurement and can also circulate the light in the bottom layer of plasmonic solar cell for producing more electron–hole pairs to improve the cell efficiency.

Acknowledgments The author acknowledges the financial support of the Deutsche Forschungsgemeinschaft (DFG FOR 845), Germany, and DST-Fast track young scientist scheme (India). The author would like to thank E. Christalle (HZDR, Germany) for SEM measurements, and A. Mücklich (HZDR, Germany) for TEM measurements. Fruitful discussion with and the support given by Dr. S. Facsko are gratefully acknowledged.

References

Amendola V, Meneghetti M (2012) Exploring how to increase the brightness of surface enhanced Raman spectroscopy

- nanolabels: the effect of the Raman-active molecules and of the label size. *Adv Funct Mater* 22(2):353–360
- Atwater HA, Polman A (2010) Plasmonics for improved photovoltaic devices. *Nat Mater* 9:205–213
- Azarian A, Zad AI, Dolati A, Ghorbani M (2008) Surface plasmon resonance of two-segmented Au–Cu nanorods. *Nanotechnology* 19:415705–415710
- Babonneau D, Camelio S, Simonot L, Pailloux F, Guérin P, Lamongie B, Lyon O (2011) Tunable plasmonic dichroism of Au nanoparticles self-aligned on rippled Al₂O₃ thin films. *EPL* 93:26005–26010
- Balci S, Karademir E, Kocabas C, Aydinli A (2011) Direct imaging of localized surface plasmon polaritons. *Opt Lett* 36(17):3401–3403
- Barnes WL, Dereux A, Ebbesen TW (2003) Surface plasmon subwavelength optics. *Nature* 424:824–830
- Brioude A, Jiang XC, Pileni MP (2005) Optical properties of gold nanorods: DDA simulations supported by experiments. *J Phys Chem B* 109:13138–13142
- Camelio S, Babonneau D, Lantiat D, Simonot L, Pailloux F (2009) Anisotropic optical properties of silver nanoparticle arrays on rippled dielectric surfaces produced by low-energy ion erosion. *Phys Rev B* 80:155434–155444
- Chern R, Liu X, Chang C (2007) Particle plasmons of metal nanospheres: application of multiple scattering approach. *Phys Rev E* 76:016609–016617
- Hsu TM, Chang CC, Hwang YF, Lee KC (1983) The dielectric function of silver by ATR technique. *Chin J Phys* 21:26–32
- Jain PK, Huang W, El-Sayed MA (2007) On the universal scaling behavior of the distance decay of plasmon coupling in metal nanoparticle pairs: a plasmon ruler equation. *Nano Lett* 7:2080–2088
- Jensen TR, Schatz GC, Duyne RPV (1999) Nanosphere lithography: surface plasmon resonance spectrum of a periodic array of silver nanoparticles by UV–Vis extinction spectroscopy and electrodynamic modelling. *J Phys Chem B* 103:2394–2401
- Johnson PB, Christy RW (1972) Optical constants of the noble metals. *Phys Rev B* 6:4370–4379
- Keller A, Facsko S, Möller W (2008) Minimization of topological defects in ion-induced ripple patterns on silicon. *New J Phys* 10:063004–063012
- Knight MW, Fan J, Capasso F, Halas NJ (2010) Influence of excitation and collection geometry on the dark field spectra of individual plasmonic nanostructures. *Opt Express* 18:2579–2587
- Koh AL, Bao K, Khan I, Smith WE, Kothleitner G, Nordlander P, Maier SA, McComb DW (2009) Electron energy-loss spectroscopy (EELS) of surface plasmons in single silver nanoparticles and dimers: influence of beam damage and mapping of dark modes. *ACS Nano* 3(10):3015–3022
- Kooij ES, Poelsema B (2006) Shape and size effects in the optical properties of metallic nanorods. *Phys Chem Chem Phys* 8:3349–3357
- Kreibig U, Vollmer M (1993) Optical properties of metal clusters (Springer series in material science)
- Krenn JR, Schider G, Rechberger W, Lamprecht B, Leitner A, Aussenegg FR, Weeber JC (2000) Design of multipolar plasmon excitations in silver nanoparticles. *Appl Phys Lett* 77:3379–3381
- Lin HY, Huang CH, Chang CH, Lan YC, Chui HC (2010) Direct near-field optical imaging of plasmonic resonances in metal nanoparticle pairs. *Opt Express* 18:165–172
- Maier SA, Kik PG, Atwater HA, Meltzer S, Harel E, Koel BE, Requicha AG (2003) Local detection of electromagnetic energy transport below the diffraction limit in metal nanoparticle plasmon waveguides. *Nat Mater* 2:229–232
- Montgomery JM, Lee TW, Gray SK (2008) Theory and modeling of light interactions with metallic nanostructures. *J Phys* 20:323201–323212
- Nie S, Emory SR (1997) Probing single molecules and single nanoparticles by surface-enhanced Raman scattering. *Science* 275:1102–1106
- Numazawa S, Ranjan M, Heinig K-H, Facsko S, Smith R (2011) Ordered Ag nanocluster structures by vapor deposition on pre-patterned SiO₂. *J Phys* 23:222203–222208
- Oates TWH, Ranjan M, Facsko S, Arvin H (2011) Highly anisotropic effective dielectric functions of silver nanoparticle arrays. *Opt Express* 19:2014–2028
- Ozbay E (2006) Plasmonics: merging photonics and electronics at nanoscale dimensions. *Science* 311:189–193
- Qian X, Peng X-H, Ansari DO, Goen QY, Chen GZ, Shin DM, Yang L, Young AN, Wang MD, Nie S (2008) In vivo tumor targeting and spectroscopic detection with surface-enhanced Raman nanoparticle tags. *Nat Biotechnol* 26:83–90
- Ranjan M, Facsko S (2012) Anisotropic surface enhanced Raman scattering in nanoparticle and nanowire arrays. *Nanotechnology* 23:485307–485313
- Ranjan M, Oates TWH, Facsko S, Möller W (2010) Optical properties of silver nanowire arrays with 35 nm periodicity. *Opt Lett* 35:2576–2578
- Ranjan M, Oates TWH, Facsko S (2012). Applications of ion induced patterned substrates in plasmonics. In: Som T, Kanjilal D (eds) *Advances in nanofabrication: from lithography to ion-beam sputtering*. ISBN 978-981-4303-75-0 (Hardback), 978-981-4303-76-7 (eBook). PanStanford Publishing, Singapore, pp 297–327
- Ranjan M, Facsko S, Fritzsche M, Mukherjee S (2013) Plasmon resonance tuning in Ag nanoparticles arrays grown on ripple patterned templates. *Microelectron Eng* 102:44–47
- Sprunken DP, Omi H, Furukawa K, Nakashima H, Sychugov I, Kobayashi Y, Torimitsu K (2007) Influence of the local environment on determining aspect-ratio distributions of gold nanorods in solution using Gans theory. *J Phys Chem C* 111:14299–14306
- Stockman MI, Kling MF, Kleineberg U, Krausz F (2007) Attosecond nanoplasmonic field microscope. *Nat Photonics* 1:539–544
- Su KH, Wei QH, Zhang X (2003) Interparticle coupling effects on Plasmon resonances of nano metallic particles. *Nano Lett* 3:1087–1090
- Sweatlock LA, Maier SA, Atwater HA, Penninkhof JJ, Polman A (2005) Highly confined electromagnetic fields in arrays of strongly coupled Ag nanoparticles. *Phys Rev B* 71:235408–235414
- Thomas R, Swathi RS (2012) Organization of metal nanoparticles for surface-enhanced spectroscopy: a difference in size matters. *J Phys Chem C* 116:21982–21991
- Toma A, Chiappe D, Massabo D, Boragno C, Mongeot FB (2008) Self-organized metal nanowire arrays with tunable optical anisotropy. *Appl Phys Lett* 93:163104–163106

- Verre R, Fleischer K, Ualibek O, Shvets IV (2012) Self-assembled broadband plasmonic nanoparticle arrays for sensing applications. *Appl Phys Lett* 100:031102–031104
- Zeng N, Murphy AB (2009) Heat generation by optically and thermally interacting aggregates of gold nanoparticles under illumination. *Nanotechnology* 20:375702–375709
- Zong RL, Zhou J, Li Q, Du B, Li B, Fu M, Qi XW, Li LT, Buddhudu S (2004) Synthesis and optical properties of silver nanowire arrays embedded in anodic alumina membrane. *J Phys Chem B* 108:16713–16716